CELL STRUCTURE AND FUNCTION *Advance Publication by J-STAGE*

doi:10.1247/csf.13017

Received on: 2013/08/08
Accepted on: 2013/10/11
Released online on: 2013/10/18

Second harmonic generation reveals collagen fibril remodeling in fibroblast-populated collagen gels

Fujio Toki[1,2,*], Naoki Honkura[4,*], Yuji Shirakata[5,7], Takeshi Imamura[3,4,7], Shigeki Higashiyama[2,6], and Daisuke Nanba[1,2]

[1]Senior Research Fellow Center, [2]Division of Cell Growth and Tumor Regulation, [3]Division of Bio-imaging, Proteo-Science Center (PROS), and [4]Department of Molecular Medicine for Pathogenesis, [5]Department of Dermatology, and [6]Department of Biochemistry and Molecular Genetics, Graduate School of Medicine, and [7]Translational Research Center, Ehime University Hospital, Ehime University, Shitsukawa, Toon, Ehime 791-0295, Japan.

* These authors contributed equally to this work.

Corresponding author:
Daisuke Nanba, Ph.D.
Senior Research Fellow Center, Ehime University, Shitsukawa, Toon, Ehime 791-0295, Japan.

Tel: +81 89 960 5254

Fax: +81 89 960 5256

E-mail: nanba.daisuke.mk@ehime-u.ac.jp

Key words: collagen, collagen gel contraction, fibroblasts, second harmonic generation, mutiphoton microscopy

Running titles: SHG imaging of collagen

Abstract

Remodeling of collagen fibrils is involved in a variety of physiological and pathological processes including development, tissue repair, and metastasis. Fibroblast-populated collagen gel contraction has been employed as a model system to investigate the collagen fibril remodeling within three-dimensional collagen matrices. Research on collagen gel contraction is also important for understanding the mechanism underlying connective tissue repair, and for design considerations for engineered tissues in regenerative medicine. Second harmonic generation (SHG) is a non-linier optical effect by which well-ordered protein assemblies, including collagen fibrils, can be visualized without any labeling, and used for a noninvasive imaging of collagen fibrils in the skin. Here we demonstrate that the remodeling of collagen fibrils in the fibroblast-populated collagen gel can be analyzed by SHG imaging with a multiphoton microscope. Two models of collagen gel contraction (freely versus restrained contraction) were prepared, and orientation of fibroblasts, density, diameter, and distribution of collagen fibrils were examined by multiphoton fluorescent and SHG microscopy. Three-dimensional construction images revealed vertical and horizontal orientation of fibroblasts in freely and restrained gel contraction, respectively. Quantitative analysis indicated that collagen fibrils were accumulated within the gel and assembled into the thicker bundles in freely but not restrained collagen gel contraction. We also found that actomyosin contractility was involved in collagen fibril remodeling. This study elucidates how collagen fibrils are remodeled by fibroblasts in collagen gel contraction, and also proves that SHG microscopy can be used for the investigation of the fibroblast-populated collagen gel.

Introduction

Collagen provides tensile strength and rigidity to connective tissues of many organs including the skin, bones, joints, muscles, and blood vessels. These mechanical properties result from the microstructure, network organization, and orientation of collagen fibrils that are the assembly of the triple-strand helical structure of fibrillar collagen molecules (Prockop and Kivirikko, 1995). Indeed, it has been found that the diameter of collagen fibrils in various tissues are correlated with the tensile strength of the tissue (Parry et al., 1978).The mechanical properties of tissues also influence lineage specification of multipotent stem cells (Engler et al., 2006; Mammoto and Ingber, 2009), and tumor cell migration (Ghajar et al., 2007; Zaman et al., 2006). Hence, the synthesis, degradation, and remodeling of collagen fibrils by connective tissue cells, including fibroblasts, osteocytes, and chondrocytes, are involved in a variety of physiological and pathological processes, and are also implicated in developmental biology, stem cell biology, and cancer biology.

Fibroblasts show the ability to contract reconstituted type I collagen gel in which they are populated (Bell et al., 1979; Grinnell and Lamke, 1984). Although the synthesis and degradation of collagen molecules do not significantly contribute to the gel contraction (Guidry and Grinnell, 1987; Mauch et al., 1988), this fibroblast-populated collagen gel has been employed as the model system to investigate the behaviors of fibroblasts within three-dimensional collagen matrices, and the remodeling of collagen fibrils by fibroblasts (Grinnell and Petroll, 2010). Now, research on collagen gel contraction has become more important for understanding the mechanisms underlying wound closure

and repair of connective tissues, and also for design considerations for engineered tissues in regenerative medicine (Brown and Phillips, 2007; Clark et al., 2007; Grinnell and Petroll, 2010; Lutolf and Hubbell, 2005).

Transmission electron microscopy has revealed that the collagen fibrils are accumulated proximal to the cells in the fibroblast-populated gel (Grinnell and Lamke, 1984). This observation has also been confirmed by reflected confocal microscopy of intact collagen fibrils (Kim et al., 2006), and confocal microscopy of fluorescein isothiocyanate (FITC)-prelabeled type I collagen (Yamato et al., 1995). However, a recent study has clearly demonstrated that the signal intensity seen by reflected confocal microscopy imaging depends on the vertical orientation of the fibrils in the gel, and that reflected confocal microscopy imaging is not suitable for yielding more complete structural information of three-dimensional collagen fibrils (Jawerth et al., 2010). In addition, the confocal images of the gel reconstructed by FITC-prelabeled type I collagen cannot exclude the signals from disassembled collagen molecules. Therefore, the quantitative assessment of the collagen fibril remodeling with other imaging modalities is required to understand the precise mechanism underlying the contraction of the fibroblast-populated collagen gel.

Second harmonic generation (SHG) is a second-order nonliner optical effect that is observed in an intense laser field. There, photons interact with noncentrosymmetric materials and are effectively combined to form new photons with twice the energy. This process results in the production of a coherent wave at exactly twice the incident frequency (Campagnola et al., 1999). SHG enables a nondestructive imaging of

well-ordered and noncentrosymmetric protein assemblies, such as collagens, microtubules, and muscle myosins (Campagnola and Loew, 2003). Collagen fibrils, higher-order polymers of fibrillar collagen molecules, produce a high SHG signal (Roth and Freund, 1979), and can be visualized in the dermis of the skin with SHG microscopy (Campagnola et al., 2002; Zipfel et al., 2003). Then, SHG has been utilized to investigate the organization of collagen fibrils in human skin from healthy volunteers (Stoller et al., 2002; Sun et al., 2006; Yasui et al., 2004), and patients with scar tissues, psoriasis, and skin tumors (Brown et al., 2003; Chen et al., 2011; Cicchi et al., 2008; Konig and Riemann, 2003; Lin et al., 2006), as a noninvasive imaging modality.

Here, we visualize collagen fibrils in the human dermal fibroblast-populated collagen gel by SHG imaging and investigate how collagen fibrils are remodeled during collagen gel contraction.

Materials and methods

Human dermal fibroblast culture

Human dermal fibroblasts were isolated from normal skin tissues, and maintained at 37^{o}C and 10% CO_2 in Dulbecco-Vogt modification of Eagle's medium (DMEM) (Invitrogen, Carlsbad, CA) containing 10% fetal bovine serum (FBS) (SAFC Biosciences, Lenexa, KS). The medium was changed every 4 days. Fibroblasts were used between passages 6 and 9.

Inhibitors and reagents

Y-27632 and cytochalasin D were purchased from Wako (Osaka, Japan), and (-)-blebbistatin from Sigma-Aldrich (St. Louis, MO). Rhodamine-phalloidin was obtained from Invitrogen.

Preparation of fibroblast-populated collagen gels

Collagen gel solution was prepared on ice by mixing Cellmatrix type I-A (acid-soluble fraction of type I collagen from bovine tendon; Nitta Gelatine, Yao, Japan): Reconstitution buffer (Nitta Gelatine): 5 x DMEM (Sigma-Aldrich) in a ratio of 7:1:2. Fibroblasts cultured until subconfluent were trypsinized, and suspended with culture medium. Cells were counted and centrifuged to prepare a suspension at a concentration of 10^6 cells/ml in DMEM. Four volumes of the collagen gel solution were added to 1 volume of the cell suspension. The final concentrations of collagen and cells were 1.68 mg/ml and $2x10^5$ cells/ml, respectively. The final mixture (500 μl /well) was added to each well of 24-well tissue culture plates (#3820-024 with normal adhesion surface and

EZ-BindShut II #4820-800LP with low adhesion surface; IWAKI, Shizuoka, Japan). After 1 hour of incubation at 37°C and 10% CO_2, 1ml per well of culture medium containing FBS was added with and without pharmacological inhibitors. The final concentrations of Y-27632, (-)-blebbistatin, and cytochalasin D were 10 μM, 10 μM, and 100 nM, respectively. After 2 days of incubation at 37°C and 10% CO_2, the collagen gel was fixed with 3.7% buffered formaldehyde phosphate-buffered saline (PBS), and observed with a multiphoton microscope.

Rhodamine-phalloidin staining

The collagen gel was fixed with 3.7% buffered formaldehyde in PBS at 4°C for 1 hour, treated with 0.1% Triton-X-100 in PBS for 10 min, and subsequently washed with PBS. The gel was then incubated with 4 units/ml rhodamine-phallodin for 30 min, and washed with PBS overnight. The stained gel was observed with a multiphoton microscope.

Multiphoton microscopy

Multiphoton imaging was performed with a galvano scanner (A1R MP; NIKON, Tokyo, Japan) giving 512x512 pixel frames at 0.5Hz by using a NIKON 25x NA 1.1 water immersion objective lens. A mode-locked infrared laser line at 950 nm was used, originating from a dispersion-corrected high power Ti-Saphire laser (Mai Tai HP DeepSee; Spectra-Physics, Tokyo, Japan) together with optical filters 483/32 for SHG (Semrock, Rochester, NY), 594LP for tetramethylrhodamine (TMR) emission (Semrock), 511LP for SHG/TMR detection splitting.

SHG imaging

The SHG signal at 475 nm was detected by a GaAsP photomultiplier tube, using a narrow-band pass filter (483/32, Semrock). The wavelength of the pumping laser was chosen to be 950 nm to minimize autofluorescence signals and suitable for TMR excitation. We set a dielectric-coated concave mirror (CM508-050-E02; Thorlabs, Newton, NJ) on the Z-axis slide stage (TSD-603; Sigma Koki, Tokyo, Japan), and searched the adjust position of concave mirror to detect SHG signals.

Image analysis

Obtained images were analyzed with Fiji (Schindelin et al., 2012). A sequence of Z-stack images was reconstituted with NIS-Elements (NIKON). The relative intensity of SHG signals was calculated by the sum of SHG signal intensity of all pixels from a single microscopic image. The experimental values were obtained from a number of images in each experiment (See Figure legends). The diameter of individual SHG signals was defined as the length of the minor axis of well-isolated each SHG signal. The experimental values were obtained from 20 SHG signals from each condition.

Statistical analysis

The values are expressed as means ± s.d.. *p* value was calculated by two-tailed Student's t-test. Values with $p < 0.05$ were considered statistically significant.

Results

Differences in the orientation of fibroblasts in floating and anchored collagen gel contraction

We developed two models of human dermal fibroblast-populated collagen gel contraction. The first model was a floating collagen gel contraction; the fibroblast-populated collagen gel was prepared in a microwell with low adhesion surface (Fig. 1A). In this model, gel contraction occurs when cell-containing gels are released from the culture surface soon after collagen polymerization (Grinnell, 2000). The other model was an anchored collagen gel contraction; the fibroblast-containing collagen gel was made in a microwell with normal adhesion surface (Fig. 1A). In the second model, restrained gel contraction occurs because the collagen gel remains attached to the plastic culture surface and cell-matrix tension are generated (Grinnell, 2000). All gels were incubated for 48 hours after prepartion. In the floating contraction model, the gel markedly decreased its diameter, however, contraction was completely inhibited in the restrained contraction model (Fig. 1B). The collagen gel without fibroblasts did not show any contractile activity, even if it was prepared in a microwell with low adhesion surface (Fig. 1B).

We first investigated whether the two distinct modes of collagen gel contraction change the organization of fibroblasts in the gels. The fibroblast-populated gels incubated for 48 hours were fixed and stained with rhodamine-phalloidin, and then cells were visualized by multiphoton fluorescent microscopy. The construction of three-dimensional images revealed vertical orientation of fibroblasts in floating collagen gels (Fig. 1C). On the

contrary, cells in adherent collagen gels were predominantly distributed along the horizontal axis, with the highest tension between fibroblasts and collagen lattice (Fig. 1D). These results indicated that human dermal fibroblasts changed their orientation in the gels by sensing cell-matrix tension.

Experimental setting for SHG imaging of the fibroblast-populated collagen gel

The collagen gel, held by an agarose gel, was mounted on the stage of an upright multiphoton microscope. In our experimental setting, the signals from specimens were detected through the objective lens (Fig. 2A and B). However, the phase-coherent SHG light has a forward propagating nature, and a transmission mode of detection is required to obtain a significant amount of SHG signals. Although the backscattering SHG light could be detected in our setting, the intensity of SHG signals of collagens in the gel was very low even if the laser power was absolutely high (Fig. 2C). To obtain better SHG images, we set a concave mirror under the collagen gel held by an agarose gel to reflect the transmitted SHG light into the objective lens (Fig. 2A and B). The gathering of transmitted and backscattering SHG light by using the mirror significantly enhanced SHG signals, which achieved the better SHG imaging of the collagen fibrils in the gel (Fig. 2C).

Remodeling of collagen fibrils in the freely and restrained collagen gel contraction

We next measured the intensity of SHG signals from collagen fibrils in floating and adherent collagen gels by SHG microscopy, which was optimized for collagen gels (Fig. 2). Whereas a large amount of SHG signals were detected in the floating gel contraction model, the signals were very faint in the anchored collagen gel contraction model (Fig.

3A). Quantitative analysis clearly revealed a 4-fold increase in SHG lights from the floating gels against those from the anchored gels (Fig. 3B). Furthermore, the anchored collagen gels showed a 2-fold increase in SHG signals against collagen gels not containing fibroblasts (Fig 3B). We next measured the diameter of individual SHG signals in each condition. The signals from the floating and anchored gels had 1.62 ± 0.335 μm (mean ± s.d.) and 1.05 ± 0.261 μm (mean ± s.d.) in diameter (Fig. 3C). When fibroblasts were not populated in the collagen gels, SHG signals were 0.778 ± 0.124 μm (mean ± s.d.) in diameter (Fig. 3C). The quantitative analysis of SHG signals revealed that human dermal fibroblasts had the ability to assemble the collagen fibrils in the gels, and that this activity was enhanced in freely collagen gel contraction.

Distribution of collagen fibrils in the freely and restrained collagen gel contraction

It has been reported that the collagen fibrils are accumulated proximal to the cells in the fibroblast-populated gel as observed by transmission electron microscopy (Grinnell and Lamke, 1984). However, it is difficult to obtain wide area images and quantitative data with this method. Therefore, we examined the distribution of collagen fibrils in freely and restrained collagen gel contraction models. The fibroblast-populated gels were fixed and stained with rhodamine-phalloidin, and then cells and collagen fibrils were visualized by multiphoton fluorescent and SHG microscopy, respectively. In the floating collagen gels, SHG signals significantly accumulated around rhodamine-positive cells (Fig. 4A). The quantitative analysis of rhodamine and SHG signals revealed that the collagen fibrils accumulated within approximately 20 μm proximal to the cells in the gels (Fig. 4A). In contrast, the accumulation of collagen fibrils around fibroblasts was not observed in the anchored collagen gels (Fig. 4B). These data clearly demonstrated

that collagen fibrils were accumulated proximal to the cells by human dermal fibroblasts in the freely contracting collagen gel.

Actomyosin contractility is required for collagen fibril remodeling

Attenuation of actin polymerization with cytochalasin B has inhibits collagen gel contraction (Nogawa and Nakanishi, 1987). Inhibition of ROCK activity has also results in the decreased contraction of the collagen gels (Kim et al., 2006). ROCK regulates both actin polymerization and MLC phosphorylation, under Rho subfamily GTPases (Amano et al., 2010; Maekawa et al., 1999). Finally, we examined whether actomyosin contractility is involved in the remodeling of collagen fibrils. ROCK inhibitor Y-27632, myosin ATPase inhibitor (-)-blebbistatin (Blebb), and actin polymerization inhibitor cytochalasin D (CytoD) reduced the contractile activity of collagen gels by fibroblasts in the floating gel (Fig. 5A). Inhibition of actomyosin contractility and actin polymerization modestly changed the angle of cells against the horizontal plane in both collagen gel contraction models (Fig. 5B). However, SHG intensity and the diameter of SHG signals were significantly decreased by treatment with Y-27632, Blebb, and CytoD in the floating, but not in the anchored, collagen gels (Fig. 5C and D). These results indicated that the assembly of collagen fibrils in freely collagen gel contraction required actomyosin contractility.

Discussion

Fibroblast-populated collagen gel contraction has been studied for more than three decades; however, the mechanism behind this process is still unclear. This is at least in part due to difficulty in visualization of collagen fibrils in three-dimensional collagen matrices. In this study, we demonstrated that SHG imaging visualized the collagen fibril network without any labeling in the gel and that the quantitative image analysis dissected remodeling of collagen fibrils in the fibroblast-populated collagen gel. This work has three major findings concerning collagen gel contraction. First, fibroblasts show vertical orientation in freely gel contraction, but are distributed along the horizontal axis in response to extracellular tension in restrained contraction. Second, collagen gel contraction involves both the accumulation of collagen fibrils proximal to the cells, and the assembly of collagen fibrils into the thicker bundles. Third, actomyosin contractility is required for the accumulation and assembly of collagen fibrils.

Concerning the mechanism of collagen gel contraction, Yamato and colleagues (Yamato et al., 1995) have hypothesized that fibroblasts extend cellular protrusions and attach collagen fibrils to them by making the collagen-integrin-cytoskeleton complexes, and that subsequent withdrawal of the protrusions results in the accumulation of collagen fibrils in the vicinity of the plasma membrane. These processes could explain collagen gel contraction by fibroblasts. In fact, attachment of collagen fibrils to cellular protrusions containing microfilaments has been observed by transmission electron microscopy (Grinnell and Lamke, 1984). Our results reinforce this hypothesis. We

demonstrated quantitatively that collagen fibrils accumulated around the fibroblasts, and assembled into the thicker bundles in freely gel contraction, which required actomyosin contractility. In anchored collagen gels, fibroblasts might not be able to draw collagen fibrils against the external tensions. We also found changes in the orientation of fibroblasts in floating and anchored collagen gels. Although the involvement of cell orientation in gel contraction was not clear, the longitudinal axis of fibroblasts was perpendicular in relation to the direction of contraction in both floating and anchored collagen gels. This means that the large surface area of the cells is available for forming cellular protrusions to accumulate collagen fibrils in the vicinity of the plasma membrane.

To validate the hypothesis described above, and comprehend the precise mechanism underlying the contraction of the fibroblast-populated collagen gel, live-imaging of fibroblasts and associated collagen fibrils in the gel is definitely crucial. The combination of multiphoton fluorescent and SHG microscopy is widely used for nondestructive imaging of living tissues (Campagnola et al., 2002; Cicchi et al., 2008; Zipfel et al., 2003). In the present study, however, the high laser power was required to detect SHG signals from collagen gels, which caused the local heating effects and damaged the fibroblasts in the gel. Systems comprising laser irradiation and SHG detection should be improved to achieve SHG live-imaging of the fibroblast-populated collagen gel.

This study showed that remodeling of collagen fibrils required actomyosin contractility of fibroblasts. We have previously demonstrated that actin filaments were remodeled

during conversion from a human epidermal keratinocyte stem cell to its progeny with restricted growth potential, and that actin filament dynamics and actomyosin contractility were involved in maintenance of keratinocyte stem cells in vitro (Nanba et al., 2013). Importantly, the difference in collagen gel contractile activity is correlated with replicative aging of fibroblasts (Bell et al., 1979). Recent studies have revealed the existence of mutipotent stem/progenitor cells in the skin dermis (Kuroda et al., 2010; Toma et al., 2001; Wong et al., 2006). Collagen gel contractile activity, an indicator of actomyosin contractility of cells, might be associated with proliferative capacity and multipotency of dermal fibroblasts. Understanding and controlling of collagen contractile ability also improve the transplantation of engineered tissue equivalents, since contractile activity of such equivalents is a recurring problem in skin-graft transplantation (MacNeil, 2007). Furthermore, mechanical loading to cutaneous wounds reduces scar formation (Gurtner et al., 2011; Wong et al., 2012). Hence, research on fibroblast-populated collagen gel contraction is definitely implicated in regenerative medicine of the skin and other organs.

In conclusion, our data demonstrated here that SHG microscopy achieved the visualization of the remodeling of collagen fibrils without any labeling in the gel, and revealed the remodeling of collagen fibrils in collagen gel contraction. These points are significant for advances in the investigation of collagen gel contraction.

Acknowledgements

We thank Dr. A.W. Amici (EPFL and CHUV, Switzerland) for critical reading of the

manuscript. This work was supported by Grant-in Aid for Scientific Research from Japan Society for the Promotion of Science (No. 24791159) to D.N.

References

Amano, M., Nakayama, M., and Kaibuchi, K. 2010. Rho-kinase/ROCK: A key regulator of the cytoskeleton and cell polarity. *Cytoskeleton (Hoboken, NJ),* **67**: 545-554.

Bell, E., Ivarsson, B., and Merrill, C. 1979. Production of a tissue-like structure by contraction of collagen lattices by human fibroblasts of different proliferative potential in vitro. *Proc. Natl. Acad. Sci. U S A,* **76**: 1274-1278.

Brown, E., McKee, T., diTomaso, E., Pluen, A., Seed, B., Boucher, Y., and Jain, R.K. 2003. Dynamic imaging of collagen and its modulation in tumors in vivo using second-harmonic generation. *Nat. Med.,* **9**: 796-800.

Brown, R.A., and Phillips, J.B. 2007. Cell responses to biomimetic protein scaffolds used in tissue repair and engineering. *Int. Rev. Cytol.,* **262**: 75-150.

Campagnola, P.J., and Loew, L.M. 2003. Second-harmonic imaging microscopy for visualizing biomolecular arrays in cells, tissues and organisms. *Nat. Biotechnol.,* **21**: 1356-1360.

Campagnola, P.J., Millard, A.C., Terasaki, M., Hoppe, P.E., Malone, C.J., and Mohler, W.A. 2002. Three-dimensional high-resolution second-harmonic generation imaging of endogenous structural proteins in biological tissues. *Biophys. J.,* **82**: 493-508.

Campagnola, P.J., Wei, M.D., Lewis, A., and Loew, L.M. 1999. High-resolution nonlinear optical imaging of live cells by second harmonic generation. *Biophys. J.,* **77**: 3341-3349.

Chen, A.C., McNeilly, C., Liu, A.P., Flaim, C.J., Cuttle, L., Kendall, M., Kimble, R.M., Shimizu, H., and McMillan, J.R. 2011. Second harmonic generation and multiphoton microscopic detection of collagen without the need for species specific antibodies.

Burns, **37**: 1001-1009.

Cicchi, R., Sestini, S., De Giorgi, V., Massi, D., Lotti, T., and Pavone, F.S. 2008. Nonlinear laser imaging of skin lesions. *J. Biophotonics,* **1**: 62-73.

Clark, R.A., Ghosh, K., and Tonnesen, M.G. 2007. Tissue engineering for cutaneous wounds. *J. Invest. Dermatol.,* **127**: 1018-1029.

Engler, A.J., Sen, S., Sweeney, H.L., and Discher, D.E. 2006. Matrix elasticity directs stem cell lineage specification. *Cell,* **126**: 677-689.

Ghajar, C.M., Suresh, V., Peyton, S.R., Raub, C.B., Meyskens, F.L., Jr., George, S.C., and Putnam, A.J. 2007. A novel three-dimensional model to quantify metastatic melanoma invasion. *Mol. Cancer Ther.,* **6**: 552-561.

Grinnell, F. 2000. Fibroblast-collagen-matrix contraction: growth-factor signalling and mechanical loading. *Trends Cell. Biol.,* **10**: 362-365.

Grinnell, F., and Lamke, C.R. 1984. Reorganization of hydrated collagen lattices by human skin fibroblasts. *J. Cell. Sci.,* **66**: 51-63.

Grinnell, F., and Petroll, W.M. 2010. Cell motility and mechanics in three-dimensional collagen matrices. *Annu. Rev. Cell. Dev. Biol.,* **26**: 335-361.

Guidry, C., and Grinnell, F. 1987. Contraction of hydrated collagen gels by fibroblasts: evidence for two mechanisms by which collagen fibrils are stabilized. *Coll. Relat. Res*., **6**: 515-529.

Gurtner, G.C., Dauskardt, R.H., Wong, V.W., Bhatt, K.A., Wu, K., Vial, I.N., Padois, K., Korman, J.M., and Longaker, M.T. 2011. Improving cutaneous scar formation by controlling the mechanical environment: large animal and phase I studies. *Ann. Surg.,* **254**: 217-225.

Jawerth, L.M., Munster, S., Vader, D.A., Fabry, B., and Weitz, D.A. 2010. A blind spot

in confocal reflection microscopy: the dependence of fiber brightness on fiber orientation in imaging biopolymer networks. *Biophys. J.,* **98**: L1-3.

Kim, A., Lakshman, N., and Petroll, W.M. 2006. Quantitative assessment of local collagen matrix remodeling in 3-D culture: the role of Rho kinase. *Exp. Cell Res.,* **312**: 3683-3692.

Konig, K., and Riemann, I. 2003. High-resolution multiphoton tomography of human skin with subcellular spatial resolution and picosecond time resolution. *J. Biomed. Opt.,* **8**: 432-439.

Kuroda, Y., Kitada, M., Wakao, S., Nishikawa, K., Tanimura, Y., Makinoshima, H., Goda, M., Akashi, H., Inutsuka, A., Niwa, A., Shigemoto, T., Nabeshima, Y., Nakahata, T., Nabeshima, Y., Fujiyoshi, Y., and Dezawa, M. 2010. Unique multipotent cells in adult human mesenchymal cell populations. *Proc. Natl. Acad. Sci. U S A,* **107**: 8639-8643.

Lin, S.J., Jee, S.H., Kuo, C.J., Wu, R.J., Lin, W.C., Chen, J.S., Liao, Y.H., Hsu, C.J., Tsai, T.F., Chen, Y.F., Dong, C.Y. 2006. Discrimination of basal cell carcinoma from normal dermal stroma by quantitative multiphoton imaging. *Opt. Lett.,* **31**: 2756-2758.

Lutolf, M.P., and Hubbell, J.A. 2005. Synthetic biomaterials as instructive extracellular microenvironments for morphogenesis in tissue engineering. *Nat. Biotechnol.,* **23**: 47-55.

MacNeil, S. 2007. Progress and opportunities for tissue-engineered skin. *Nature,* **445**: 874-880.

Maekawa, M., Ishizaki, T., Boku, S., Watanabe, N., Fujita, A., Iwamatsu, A., Obinata, T., Ohashi, K., Mizuno, K., and Narumiya, S. 1999. Signaling from Rho to the actin

cytoskeleton through protein kinases ROCK and LIM-kinase. *Science,* **285**: 895-898.

Mammoto, A., and Ingber, D.E. 2009. Cytoskeletal control of growth and cell fate switching. *Curr. Opin. Cell Biol.,* **21**: 864-870.

Mauch, C., Hatamochi, A., Scharffetter, K., and Krieg, T. 1988. Regulation of collagen synthesis in fibroblasts within a three-dimensional collagen gel. *Exp. Cell Res.,* **178**: 493-503.

Nanba, D., Toki, F., Matsushita, N., Matsushita, S., Higashiyama, S., and Barrandon, Y. 2013. Actin filament dynamics impacts keratinocyte stem cell maintenance. *EMBO Mol. Med.,* **5**: 640-653.

Nogawa, H., and Nakanishi, Y. 1987. Mechanical aspects of the mesenchymal influence on epithelial branching morphogenesis of mouse salivary gland. *Development,* **101**: 491-500.

Parry, D.A., Barnes, G.R., and Craig, A.S. 1978. A comparison of the size distribution of collagen fibrils in connective tissues as a function of age and a possible relation between fibril size distribution and mechanical properties. *Proc. R. Soc. Lond. B Biol. Sci.,* **203**: 305-321.

Prockop, D.J., and Kivirikko, K.I. 1995. Collagens: molecular biology, diseases, and potentials for therapy. *Annu. Rev. Biochem.,* **64**: 403-434.

Roth, S., and Freund, I. 1979. Second harmonic generation in collagen. *J. Chem. Phys.,* **70**: 1637-1643.

Schindelin, J., Arganda-Carreras, I., Frise, E., Kaynig, V., Longair, M., Pietzsch, T., Preibisch, S., Rueden, C., Saalfeld, S., Schmid, B., Tinevez, J.Y., White, D.J., Hartenstein, V., Eliceire, K., Tomancak, P., and Cardona, A. 2012. Fiji: an open-source platform for biological-image analysis. *Nat. Methods.,* **9**: 676-682.

Stoller, P., Reiser, K.M., Celliers, P.M., and Rubenchik, A.M. 2002. Polarization-modulated second harmonic generation in collagen. *Biophys. J.,* **82**: 3330-3342.

Sun, Y., Chen, W.L., Lin, S.J., Jee, S.H., Chen, Y.F., Lin, L.C., So, P.T., and Dong, C.Y. 2006. Investigating mechanisms of collagen thermal denaturation by high resolution second-harmonic generation imaging. *Biophys. J.,* **91**: 2620-2625.

Toma, J.G., Akhavan, M., Fernandes, K.J., Barnabe-Heider, F., Sadikot, A., Kaplan, D.R., and Miller, F.D. 2001. Isolation of multipotent adult stem cells from the dermis of mammalian skin. *Nat. Cell Biol.,* **3**: 778-784.

Wong, C.E., Paratore, C., Dours-Zimmermann, M.T., Rochat, A., Pietri, T., Suter, U., Zimmermann, D.R., Dufour, S., Thiery, J.P., Meijer, D., Beemann, F., Barrandon, Y., and Dommer, L. 2006. Neural crest-derived cells with stem cell features can be traced back to multiple lineages in the adult skin. *J. Cell Biol.,* **175**: 1005-1015.

Wong, V.W., Rustad, K.C., Akaishi, S., Sorkin, M., Glotzbach, J.P., Januszyk, M., Nelson, E.R., Levi, K., Paterno, J., Vial, I.N., Kuang, A.A., Longaker, M.T., and Gurtner, G.C. 2012. Focal adhesion kinase links mechanical force to skin fibrosis via inflammatory signaling. *Nat. Med.,* **18**: 148-152.

Yamato, M., Adachi, E., Yamamoto, K., and Hayashi, T. 1995. Condensation of collagen fibrils to the direct vicinity of fibroblasts as a cause of gel contraction. *J. Biochem.,* **117**: 940-946.

Yasui, T., Tohno, Y., and Araki, T. 2004. Characterization of collagen orientation in human dermis by two-dimensional second-harmonic-generation polarimetry. *J. Biomed. Opt.,* **9**, 259-264.

Zaman, M.H., Trapani, L.M., Sieminski, A.L., Mackellar, D., Gong, H., Kamm, R.D.,

Wells, A., Lauffenburger, D.A., and Matsudaira, P. 2006. Migration of tumor cells in 3D matrices is governed by matrix stiffness along with cell-matrix adhesion and proteolysis. *Proc. Natl. Acad. Sci. U S A,* **103**: 10889-10894.

Zipfel, W.R., Williams, R.M., Christie, R., Nikitin, A.Y., Hyman, B.T., and Webb, W.W. 2003. Live tissue intrinsic emission microscopy using multiphoton-excited native fluorescence and second harmonic generation. *Proc. Natl. Acad. Sci. U S A,* **100**: 7075-7080.

Figure Legends

Fig. 1

Freely and restrained collagen gel contraction. (A) A schematic drawing of two models of fibroblast-populated collagen gel contraction. Freely collagen gel contraction occurs when the gel is prepared in a well of 24-well plate with low adhesion surface. Restrained gel contraction occurs when the gel is prepared in a well with normal adhesion surface that remains attached the gel to the culture surface. (B) Photograph of gels after 2 days incubation. Air bubbles remained within the gel without cells. (C and D) Left panel shows three-dimensional reconstruction images of fibroblasts in the floating (C) and anchored (D) collagen gel. The gel was fixed and stained with rhodamine-phalloidin to visualize cells. Right panel shows distribution of angles of the longitudinal axis of fibroblasts against the horizontal plane in the floating (C) and anchored (D) collagen gel. The distributions were obtained from 33 and 36 cells in C and D, respectively. Bars, 100 μm.

Fig. 2

Experimental setting for SHG imaging of the fibroblast-populated collagen gel. (A) A schematic diagram of our mutiphoton microscope for the collagen gel SHG imaging. (B) Photograph of our experimental setting. A concave mirror was set under the collagen gel held by an agarose gel. (C) Left panel shows the SHG images of the floating collagen gels with and without the concave mirror. Right panel shows quantitative analysis of SHG intensity in each condition. The values were obtained from 9 images from each condition. Bar, 100 μm. ***, $p < 0.001$. *p* value was calculated by

two-tailed Student's t-test.

Fig. 3

Quantitative analysis of SHG signals from floating and anchored collagen gels. (A) Three-dimensional reconstruction of SHG images of floating and anchored collagen gels. Bars, 50 μm. (B) Quantitative analysis of SHG intensity in each condition. The values were obtained from 33 images from each condition. (C) Quantitative analysis of diameter of SHG signals in each condition. The values were obtained from 20 collagen fibrils from each condition. **, $P < 0.01$. ***, $p < 0.001$. *p* value was calculated by two-tailed Student's t-test.

Fig. 4

Distribution of collagen fibrils and fibroblasts in floating and anchored collagen gels. (A and B) Quantitative analysis of three-dimensional reconstruction of SHG and multiphoton fluorescent images of floating (A) and anchored (B) collagen gels. Fibroblasts were visualized by rhodamine-phalloidin staining.

Fig. 5

Effects of inhibition of actomyosin contractility on collagen fibril remodeling. (A) Inhibition of freely collagen gel contraction by Y-27632 (10 μM), (-)-blebbistatin (Blebb) (10 μM), and cytochalasin D (CytoD) (100 nM). (B) Distribution of angles of the longitudinal axis of fibroblasts against the horizontal plane in the floating (left) and anchored (right) collagen gel in the presence of inhibitors. The distributions were

obtained from at least 10 cells from each condition. (C) Quantitative analysis of SHG intensity in the presence of inhibitors. The values were obtained from at least 11 images from each condition. (C) Quantitative analysis of diameter of SHG signals in the presence of inhibitors. The values were obtained from 20 collagen fibrils from each condition. *, $p < 0.05$, **, $p < 0.01$, and ***, $p < 0.001$ for the difference between control *versus* each inhibitor. *p* value was calculated by two-tailed Student's t-test.

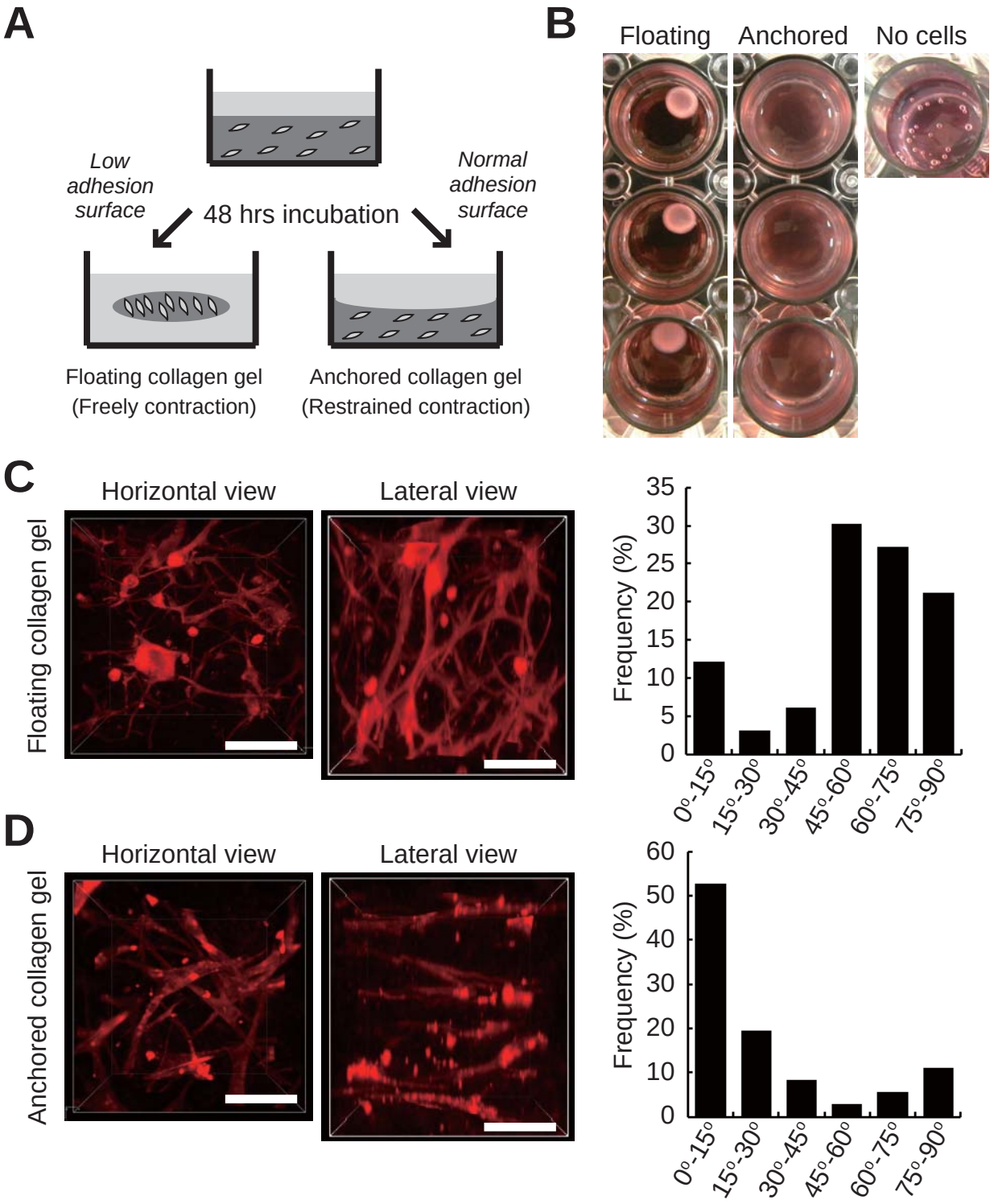
A
Low adhesion surface
48 hrs incubation
Normal adhesion surface
Floating collagen gel (Freely contraction)
Anchored collagen gel (Restrained contraction)
B
Floating
Anchored
No cells
C
Horizontal view
Lateral view
Floating collagen gel
Frequency (%)
0°-15°
15°-30°
30°-45°
45°-60°
60°-75°
75°-90°
D
Horizontal view
Lateral view
Anchored collagen gel
Frequency (%)
0°-15°
15°-30°
30°-45°
45°-60°
60°-75°
75°-90°

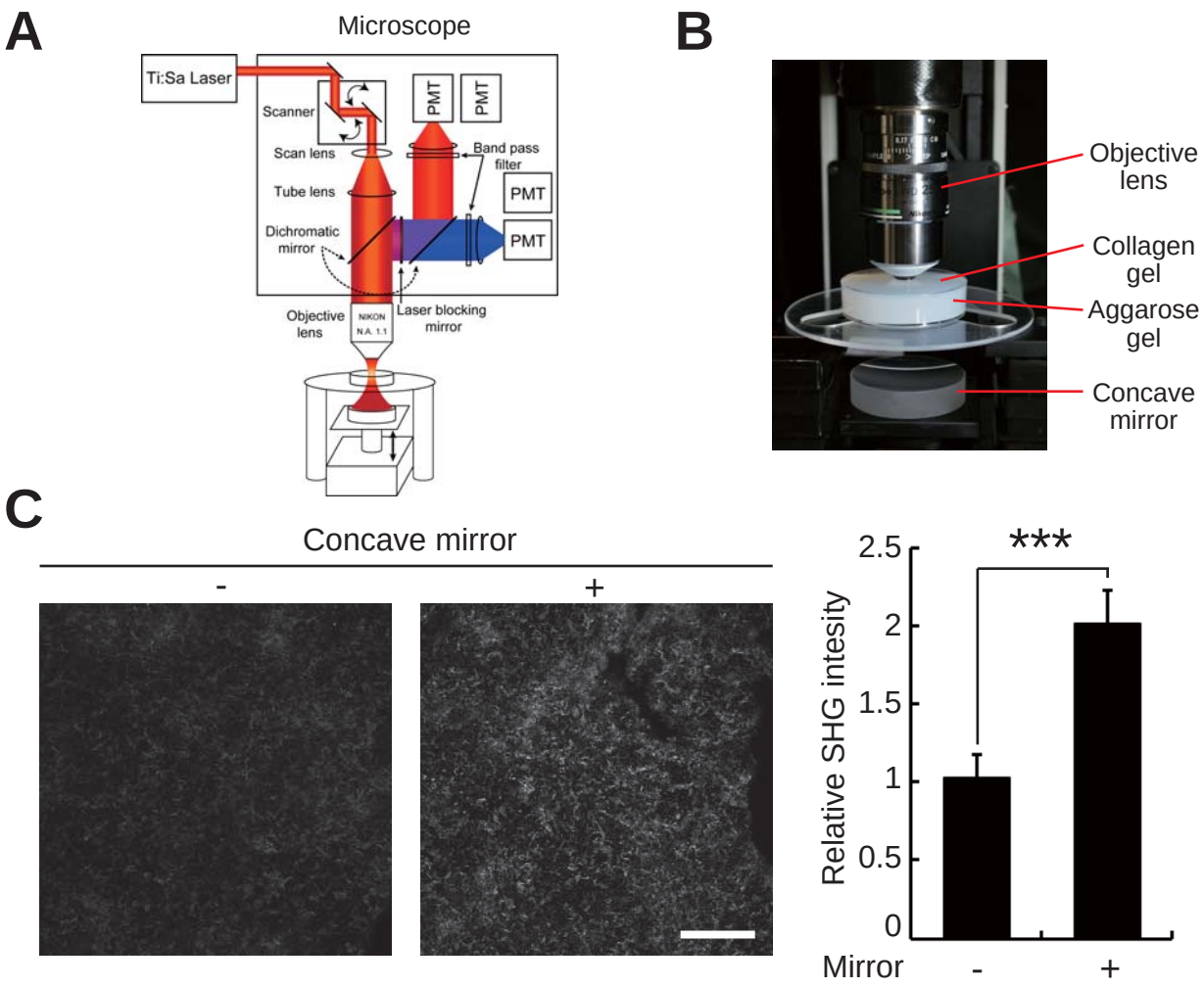
A
Microscope
Ti:Sa Laser
Scanner
PMT
PMT
Scan lens
Band pass filter
Tube lens
PMT
Dichromatic mirror
PMT
Objective lens
NIKON N.A. 1.1
Laser blocking mirror
B
Objective lens
Collagen gel
Aggarose gel
Concave mirror
C
Concave mirror
-
+
***
Relative SHG intesity
2.5
2
1.5
1
0.5
0
Mirror
-
+

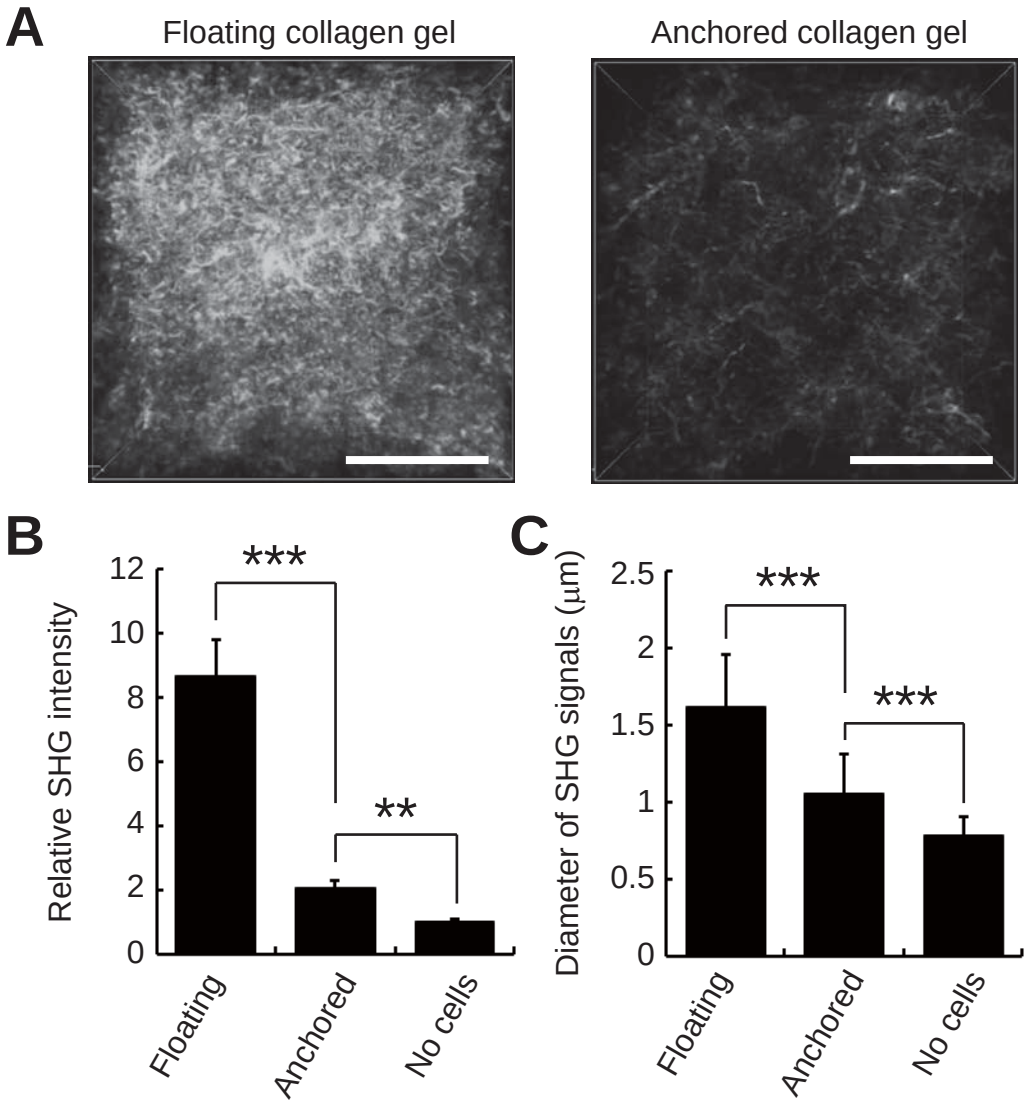
A
Floating collagen gel
Anchored collagen gel
B
Relative SHG intensity
12
10
8
6
4
2
0
***
**
Floating
Anchored
No cells
C
Diameter of SHG signals (μm)
2.5
2
1.5
1
0.5
0
***
***
Floating
Anchored
No cells

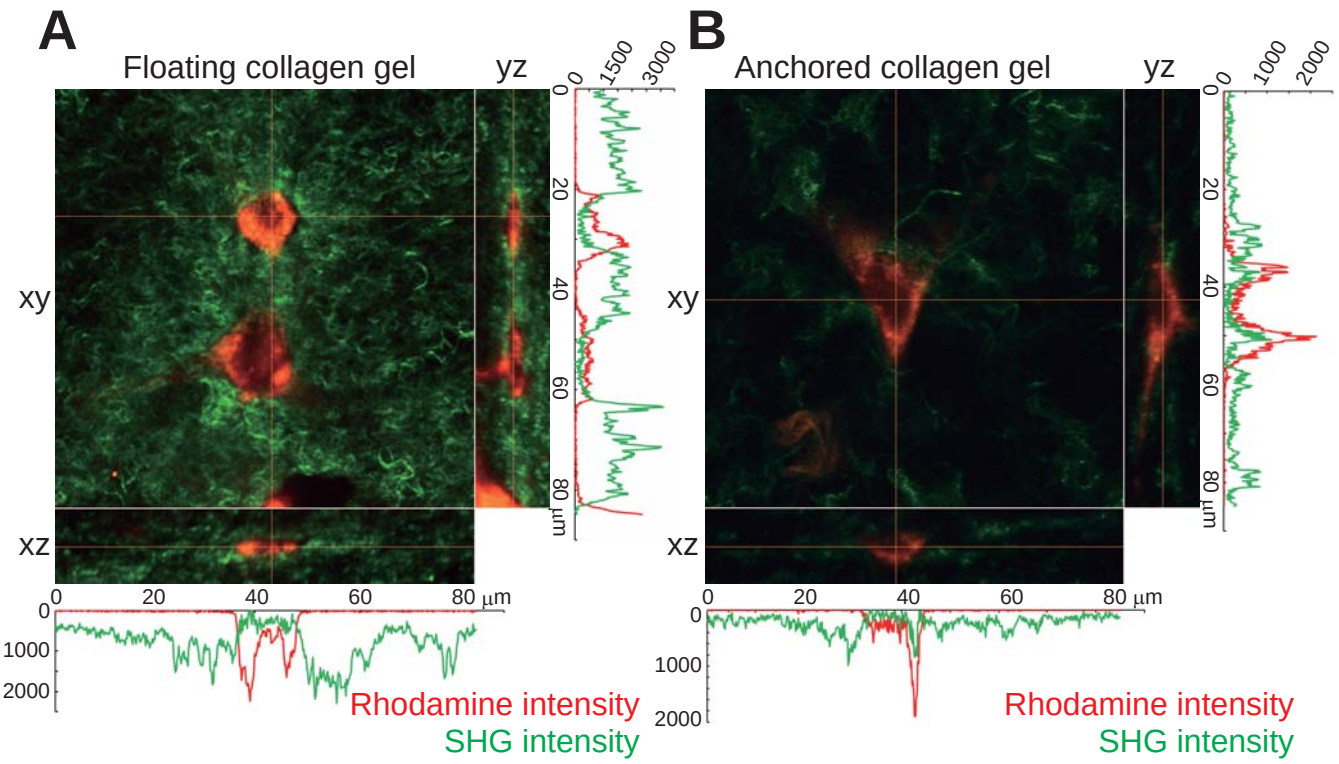
A
Floating collagen gel
yz
xy
xz
0
20
40
60
80 μm
0
1500
3000
0
1000
2000
Rhodamine intensity
SHG intensity
B
Anchored collagen gel
yz
xy
xz
0
20
40
60
80 μm
0
1000
2000
Rhodamine intensity
SHG intensity

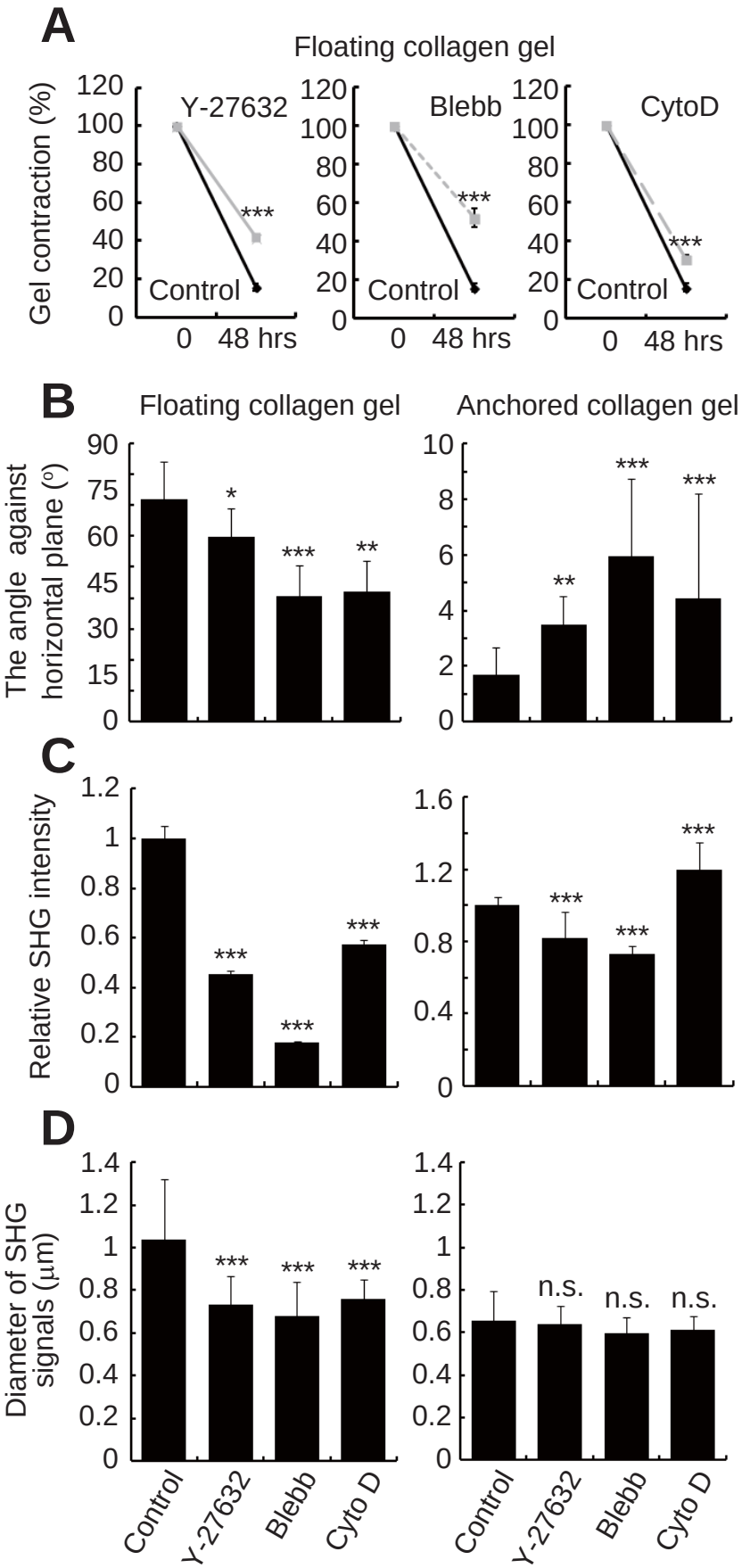
A
Floating collagen gel
Gel contraction (%)
Y-27632
Blebb
CytoD
Control
***
0
48 hrs
B
Floating collagen gel
Anchored collagen gel
The angle against horizontal plane (°)
*
**
C
Relative SHG intensity
D
Diameter of SHG signals (μm)
n.s.
Control
Y-27632
Blebb
Cyto D